

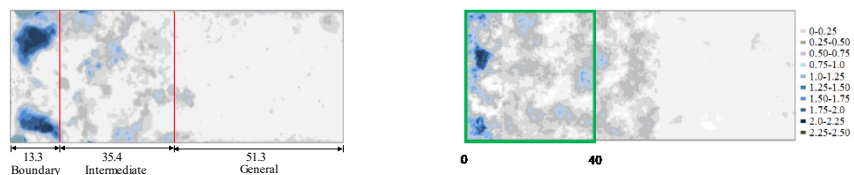
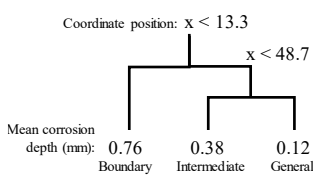
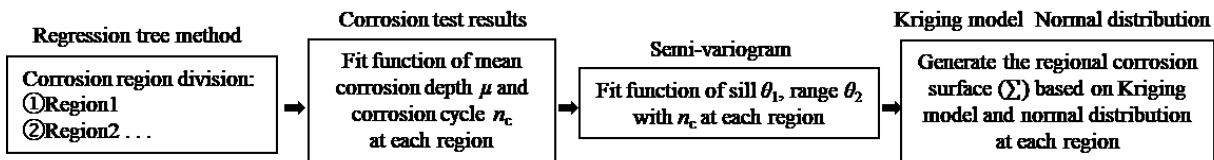
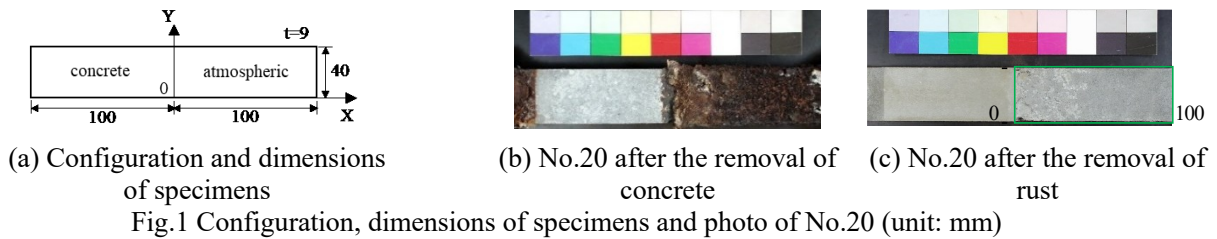
Comparison of stress concentration factor between actual and predicted corrosion surface configurations by spatial statistics simulation

Kyushu University Student Member ○Weikun XU Kyushu University Fellow Member Shigenobu KAINUMA
 Kyushu University Regular Member Muye YANG

1. Introduction In this study, the accelerated corrosion testing¹⁾ was conducted to obtain the corroded surface figuration of specimens, and the long-term corroded surfaces were simulated respectively to quantifiably identify the irregularities of the corroded surface depending on various corrosion cycles. Furthermore, the stress concentration factors of each specimen under different corrosion cycles were discussed using both test and simulation results to verify the properness of the estimation from a mechanic perspective.

2. Simulation result A total of 20 steel plates (JIS G 3106 SM490) which thickness is 9 mm, were prepared for the accelerated exposure test. Fig.1(a) shows the configuration and dimensions of specimens as well as the measuring coordinate system. The left and right part of the steel plate is embedded in the concrete block and exposed to the atmosphere respectively to simulate the boundary region between the atmospheric and concrete environment. Accelerated exposure tests were conducted according to the JIS K5600-7-9. The test specimens were tilted by about 15 degrees to the vertical direction during the exposure test. Moreover, 20 specimens were numbered from 1~20 and divided into four groups of five specimens, which was performed in the salt spray test machine for 600, 1200, 1800, and 2400 cycles, respectively. Fig.1(b) and (c) show the photo of No.20 after the removal of concrete, and after the removal of rust. The surface exposed to the atmospheric environment was chosen as the analysis area and measured by a laser focus scanning system with a 0.2 mm pitch interval. Fig.2 shows the simulation flow²⁾. The regression tree method is mainly determined by deviance D , and divided areas could be regarded as regions with different surface characteristics. Nevertheless, complexity parameter C_p is conducted to avoid excessive division, which may cause difficulty in identifying corrosion behavior. In this study, C_p was set to 0.01 to ensure even the general corrosion area can be divided at least one time. Fig.3 shows the regression tree of No.20 after 2400 cycles, and the value at every branch means the mean corrosion depth of each region. According to the significant difference in mean corrosion depth at each region, we believe that these three regions indicate three different surface characteristics and define them as the boundary, intermediate, and general area, respectively, as shown in Fig.4(a). From the corrosion depth contour in Fig.4(b), the corroded surfaces are effectively generated. However, as the maximum corrosion position generated randomly during simulation, it shows the different localized corrosion distribution in actual and simulation results.

3. FE model The mechanic model analysis is performed by establishing elastic FE models in Marc Mentat 2017, to verify the rationality of simulation results in structural aspects. The stress concentration is one of the most critical characterizations caused by corrosion damages. Thus, according to input the actual and simulated corrosion surface to FEM, the stress concentration factor (hereafter, SCF) under an axial tensile force was calculated. All models are established based on 10 specimens that show serious localized corrosion at the boundary area. Besides, these specimens showed a



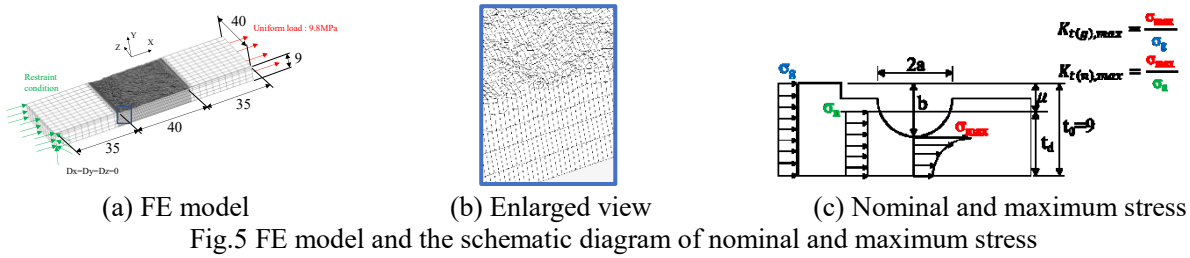


Fig.5 FE model and the schematic diagram of nominal and maximum stress

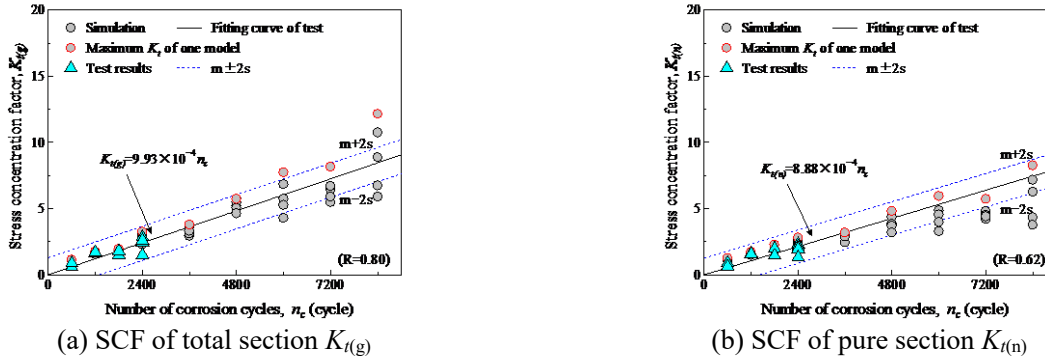


Fig.6 Stress concentration factor of steel plates with actual and simulated surfaces

similar region division with No.20. In this study, each model is composed of 8 nodes elements. To evaluate the stress concentration condition, one specific area of either actual or simulated corrosion surface should be introduced and inserted into each model. According to the corrosion surface of corroded specimen exposed after 600~2400 cycles, a 0~40 mm range is selected as shown in Fig.4(b). The minimum element size of the model is determined to be 0.4×0.4×0.4mm as the corrosion insert surface of the model is produced by extracting 0.4 mm pitch data from the data of the corrosion depth of the test specimen. After this, the corrosion surface is inserted into the model using the R program. Furthermore, to ensure the accuracy of the stress distribution, the elements near the corrosion surface are densely divided along the thickness direction of the model, as shown in Fig.5(b). Fig.5(a) shows the boundary conditions and image of the model (110×40×9mm). A uniform load of 9.8 MPa and displacement constraint ($D_x=D_y=D_z=0$) are applied to two ends of the longitudinal direction. Fig.5(c) shows the schematic diagram of nominal and maximum stress. σ_{max} , σ_g , and σ_n mean the maximum stress of one corrosion hole, the nominal stress of cross-section without corrosion, and the nominal stress of cross-section with mean corrosion depth, in the x-direction, respectively. Herein, $K_{t(g)}$, $K_{t(n)}$ are introduced to evaluate the mechanical properties of steel plates with both actual and simulated corrosion surface as shown in Fig.5(c). Where $K_{t(g)}$ indicates the SCF considering both effects of localized corrosion holes and reduction of plate thickness, while $K_{t(n)}$ only considers the effects of localized corrosion holes. Thus, $K_{t(g)}$, $K_{t(n)}$ are called SCF of total section and pure section, respectively. Fig.6 shows the relationship between $K_{t(g)}$ ($K_{t(n)}$) and n_c . To obtain the trend of $K_{t(g)}$ ($K_{t(n)}$) based on simulation results after 2400 cycles, 6 more models are established based on No.20 with 3600, 4800, 6000, 7200, and 8400 cycles, respectively. The largest five values of $K_{t(g)}$ ($K_{t(n)}$) are extracted from each model as shown in Fig.6. To compare the difference between test and simulation results, the linear function fitting curve of n_c and $K_{t(g)}$ ($K_{t(n)}$) based on the test results is carried out, and the dash lines refer to the 95% confidence interval of the fitting curves. The correlation coefficient R of $K_{t(g)}$ is about 0.80, while the correlation coefficient of $K_{t(n)}$ is relatively low. From the scatters before 2400 cycles, $K_{t(g)}$ ($K_{t(n)}$) based on simulated corrosion surfaces are all within the 95% confidence interval of the fitting curves and highly coinciding with that of test results. Therefore, it could be considered the simulated corrosion surfaces show a similar stress concentration effect to the actual corrosion surfaces before 2400 cycles. From 4800 cycles, the largest five values of $K_{t(g)}$ ($K_{t(n)}$) given by simulated corrosion surfaces tend to be more dispersed over time. It should be noticed that the maximum K_t of each model, as shown the red circular marks in Fig.5, are almost within the 95% confidence interval, whereas the $K_{t(g)}$ of simulated corrosion surfaces in prediction after 8400 cycles tend to be larger than actual. In general, $K_{t(g)}$ ($K_{t(n)}$) all meet the prediction curve of SCF generated from experimental data. From the results above, it is indicated that although localized corrosion holes generated by simulation distribute differently, the simulated corrosion surfaces follow the same localized corrosion tendency and show similar stress concentration effect to the actual corrosion surface.

4. Summary 1) The simulated corrosion surface of steel plates are effectively generated based on spatial statistical technique. 2) Although localized corrosion holes generated by simulation distribute differently, the simulated corrosion surfaces follow the same localized corrosion tendency and show similar stress concentration effect to the actual corrosion surface.

Reference 1) S. Kainuma and N. Hosomi: Fatigue Life Evaluation of Corroded Structural Steel Members in Boundary with Concrete, International Journal of Fracture 158 (2009) 149-158. 2) J.A. Nelder, R.W.M. Wedderburn. Generalized linear models. Journal of the Royal Statistical Society: Series A (General) 135 (1972) 370-384.